Catalysis Letters Vol. 106, Nos. 3–4, February 2006 (© 2006)
DOI: 10.1007/s10562-005-9627-z

Synthesis of vanadium phosphate catalysts by hydrothermal method for selective oxidation of *n*-butane to maleic anhydride

Y. H. Taufiq-Yap[a,*], A. R. Mohd. Hasbi[a], M. Z. Hussein[a], G. J. Hutchings[b], J. Bartley[b], and N. Dummer[b]

[a]*Department of Chemistry, Universiti Putra Malaysia, Serdang, Selangor, 43400 UPM, Malaysia*
[b]*School of Chemistry, Cardiff University, P.O. Box 912, Cardiff CF10 3TB, UK*

Received 6 October 2005; accepted 4 November 2005

Two vanadium phosphate catalysts (VPH1 and VPH2) prepared via hydrothermal method are described and discussed. Both catalysts exhibited only highly crystalline pyrophosphate phase. SEM showed that the morphologies of these catalysts are in plate-like shape and not in the normal rosette-type clusters. Temperature-programmed reduction in H_2 resulted two reduction peaks at high temperature in the range of 600–1100 K. The second reduction peak appeared at 1074 K occurred as a sharp peak indicated that the oxygen species originated from V^{4+} phase are having difficulty to be removed and their nature are less reactive compared to other methods of preparation. Modified VPH2 gave better catalytic performance for *n*-butane oxidation to maleic anhydride contributed by a higher BET surface area, high mobility and reactivity of the lattice oxygen associated to the V^{4+} which involved in the hydrocarbon's activation. A slight increased of the V^{5+} phase also enhanced the activity of the VPH2 catalyst.

KEY WORDS: vanadium phosphate; hydrothermal; butane oxidation; lattice oxygen.

1. Introduction

Vanadium phosphorus oxide (VPO) is versatile catalytic component that has been extensively applied in selective oxidation of *n*-butane to produce maleic anhydride (MA). Most attention has focused on the hemihydrate precursor phase, $VOHPO_4 \cdot 0.5H_2O$, which is transformed under reaction conditions to give a complex mixture of V^{4+} and V^{5+} phases.

To date, a number of variations of $VOHPO_4 \cdot 0.5H_2O$ formation have been documented which included (i) VPA, prepared by using the standard aqueous HCl method followed by water extraction step; (ii) VPO, prepared by the reaction of V_2O_5 with H_3PO_4 in isobutanol followed by water extraction step; (iii) VPD, prepared by the reaction of $VOPO_4 \cdot 2H_2O$ with isobutanol [1,2], (iv) sonochemical method, using ultrasound and microwave irradiation [3] and (v) using surfactants, reacting V_2O_5 and H_3PO_4 with cetyltrimethylammonium chloride [4]. However, there has been little interest in the preparation of vanadyl pyrophosphate catalyst using hydrothermal synthesis. Previous studies by Torardi *et al.* [5] and Bartley *et al.* [6] have reported the preparation of $(VO)_2P_2O_7$ catalyst by hydrothermal synthesis using V_2O_4 and H_3PO_4 as starting materials. Bartley *et al.* [6] reported that the selectivity to MA for the hydrothermal prepared catalyst (22 h for crystallization time in autoclave) was similar to other non-promoted VPO catalysts and also gave higher space time yield than that of catalysts prepared using alcohol as solvent.

In this study, vanadium phosphate catalysts were prepared via two different procedures using hydrothermal method. It highlights the development of an improved hydrothermal method for the synthesis of this catalyst. The physico-chemical properties of these catalysts synthesized using V_2O_5 as a starting material were investigated by means of various techniques, i.e., XRD, BET, SEM, O_2-TPD and TPR. The catalytic property of both catalysts will also be reported.

2. Experimental

2.1. Catalysts preparation

The $(VO)_2P_2O_7$ catalysts were prepared using different procedures of hydrothermal method with the same starting material. The first method was carried out according to the procedure proposed by Fraztky *et al.* [7]. The precursor obtained was denoted as PVPH1. Another preparation procedure was used to prepare this catalyst by using V_2O_5 (7.3 g from Fluka),*o*-H_3PO_4 (5.4 mL, 85% from Merck), oxalic acid dihydrate (7.5 g from Merck) and water (16 mL) as a mineralizer. The starting material and mineralizer were mixed uniformly before was charged into a Teflon-lined stainless steel autoclave. The hydrothermal synthesis was conducted at 423 K for 144 h. After the autoclave was cooled, the powder was centrifuged, washes with deionized water, and dried at ~373 K for 5 h. The precursor obtained was denoted as PVPH2.

* To whom correspondence should be addressed.
E-mail: yap@fsas.upm.edu.my

Both precursors were then calcined in a reaction flow of *n*-butane/air mixture (0.75% *n*-butane/air) for 6 h at 713 and 733 K, respectively. The catalysts obtained were denoted as VPH1 and VPH2.

2.2. Catalysts characterization

XRD analyses were carried out using a Shimadzu diffractometer model XRD-6000 employingCu K_α radiation to generate diffraction patterns at ambient temperature.

BET surface area was done by using a Thermo-Finnigan Sorptomatic Instrument model 1900 nitrogen adsorption/desorption at 77 K.

The average oxidation states of vanadium in the catalysts were determined by redox titration following the method of Niwa and Murakami [8].

A Jeol JSM-6400 scanning electron microscope (SEM) was used to obtain topographical information from the catalysts.

Temperature-programmed desorption (TPD) and Temperature-programmed reduction (TPR) experiments were performed by using ThermoFinnigan TPD/R/O 1100 Series instrument.

2.3. Catalytic test

The oxidation of *n*-butane to maleic anhydride was carried out in a fixed-bed flow microreactor containing a standard mass of catalyst (0.25 g) at 673 K with GHSV of 2400 h^{-1}. Prior to use, the catalysts were pelleted and sieved to give particles (250–300 μm in diameter). *n*-Butane and air were fed to the reactor via calibrated mass flow controllers to give a feedstock composition of 1.7% *n*-butane in air. The products were fed via heated lines to an on-line gas chromatography for product analysis. The reactor comprised a stainless steel tube with the catalyst held in place by plugs of quartz wool. A thermocouple was located in the centre of the catalyst bed and temperature control was typically ± 1 K. Carbon mass balances of ≥95% were typically observed.

3. Results and discussion

3.1. X-Ray diffraction

XRD patterns of the precursors (figure 1) prepared throughout both routes gave highly crystalline and exposure of the crystallographic phase (001) and in good agreement with those reported for $VOHPO_4 \cdot 0.5H_2O$ phase [1,2]. Interestingly, no traces of $VO(H_2PO_4)_2$, an impurity noted to be readily formed under traditional aqueous preparation conditions [9] was observed.

The XRD patterns (figure 2) for both catalysts (VPH1 and VPH2) showed well-crystalline materials with the same structured characterized by sharp peaks appeared at $2\theta = 23.0°$, 28.35° and 29.83° correspond to (020), (204) and (221) plane reflections, respectively.

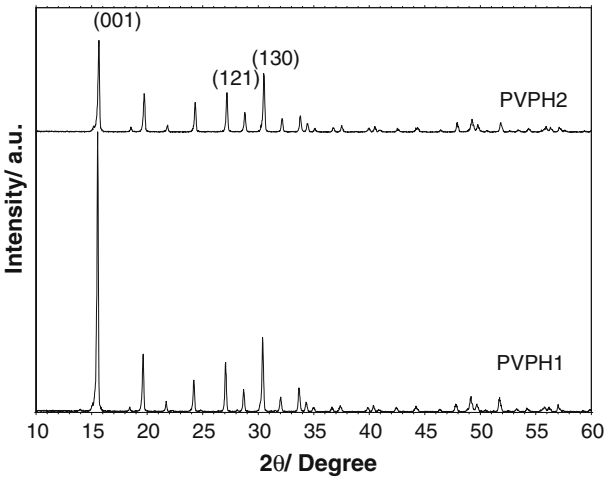

Figure 1. X-ray diffraction patterns of PVPH1 and PVPH2.

These results are in agreement with the report for vanadyl pyrophosphate phase by Kiely *et al.* [2]. The (020) plane reflection for both catalysts were more intense and narrower compared to other methods of preparation [1,2,10,11]. The particles thicknesses were such calculated using Debye–Scherrer equation [12] shows that VPH2 has smaller particles than the VPH1 catalyst.

The value of the crystallite size was summarised in table 1. The line width increases with the decreasing size of the crystallites. The crystallite sizes obtained by observations from SEM micrograph were larger than those obtained from theoretical calculation using the Debye–Scherrer equation, attributing to the presence of polycrystallinity in the particle.

3.2. BET surface area measurement and volumetric titration

The specific surface area for VPH2 (9.5 $m^2\ g^{-1}$) is slightly higher than VPH1 catalyst (8 $m^2\ g^{-1}$). These values are higher than those reported for VPO catalyst

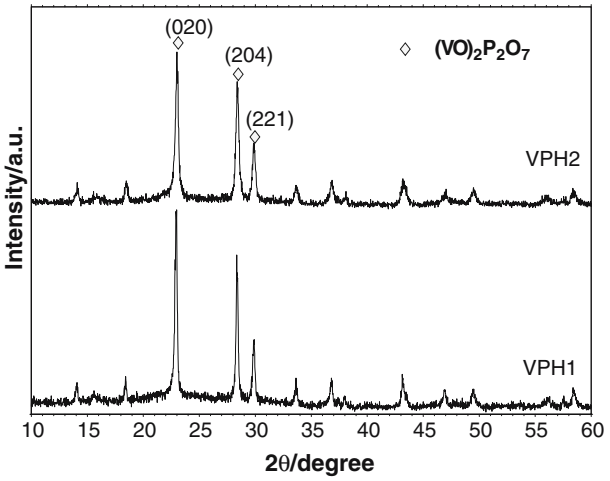

Figure 2. X-ray diffraction patterns of VPH1 and VPH2 catalysts.

Table 1
XRD data for VPH1 and VPH2 catalysts

Catalysts	Line width[a] (020)	Line width[b] (204)	Thickness[c] (020)/Å	Thickness[c] (204)/Å
VPH1	0.2337	0.2083	347.30	394.01
VPH2	0.3042	0.3188	266.84	257.37

[a] FWHM of (020) reflection.
[b] FWHM of (204) reflection.
[c] Plate thickness by means of Scherer's formula: $T(\text{Å}) = (0.9 \times \lambda)/(\text{FWHM} \times \cos\theta)$.

prepared via aqueous method [2,11]. However, the value obtained was lower than the organic [10] and dihydrate methods [11]. Recently, Bartley *et al.* [6] reported that the surface area of vanadium phosphate derived from hydrothermal synthesis using V_2O_4 as vanadium source was slightly higher *i.e.* 11 m^2g^{-1}. As mentioned previously, the BET surface area value is in accordance with the crystallite size distribution which indicates large crystallite size gives low surface area. So, from the crystallite size result calculated using Debye–Scherrer equation, VPH2 catalyst with smaller particle size gave a higher surface area compared to VPH1.

The average oxidation state of vanadium for VPH1 is 4.23. This is roughly similar for the catalyst prepared via VPD method but higher from VPO method and lower than VPA catalyst [11]. However, for VPH2, the value is higher, i.e. 4.35 which show an increased of V^{5+} phase from 23% (VPH1) to 35% (VPH2) (table 2).

3.3. Scanning electron microscopy (SEM)

Figure 3 (a and b) show the surface morphologies of the hydrothermal synthesized catalysts. VPH2 catalyst shows a small plate-like texture, whereas VPH1 catalysts illustrate the formation of larger with irregular flaky shape. These morphologies are different from the common images for vanadyl pyrophosphate catalysts, i.e. a rosette-like clusters [1,10,11]. A lower surface area obtained from these hydrothermally synthesized catalysts may due to the bulk morphologies of these catalysts.

3.4. Temperature-programmed desorption of O_2 (O_2-TPD)

The oxygen desorption spectra shown in figure 4 were obtained by pretreating the catalysts by heating them to 673 K in an oxygen flow (101 kPa, 25 cm^3 min^{-1}) and holding them under that flow at 673 K for 1 h before cooling them to ambient temperature. The high-temperature pretreatment in flowing oxygen removed any trace of water from the system. The flow was then switched to helium (1 bar, 25 cm^3 min^{-1}) and the temperature was raised (10 K min^{-1}) to 1173 K following the conductivity of oxygen by a thermal conductivity detector.

Table 2
BET surface areas and average oxidation numbers with percentages of V^{4+} and V^{5+} oxidation states present in VPH1 and VPH2

Catalysts	S_{BET} (m^2 g^{-1})	Average oxidation state of vanadium	V^{4+} (%)	V^{5+} (%)
VPH1	8	4.23	77	23
VPH2	9.5	4.35	65	35

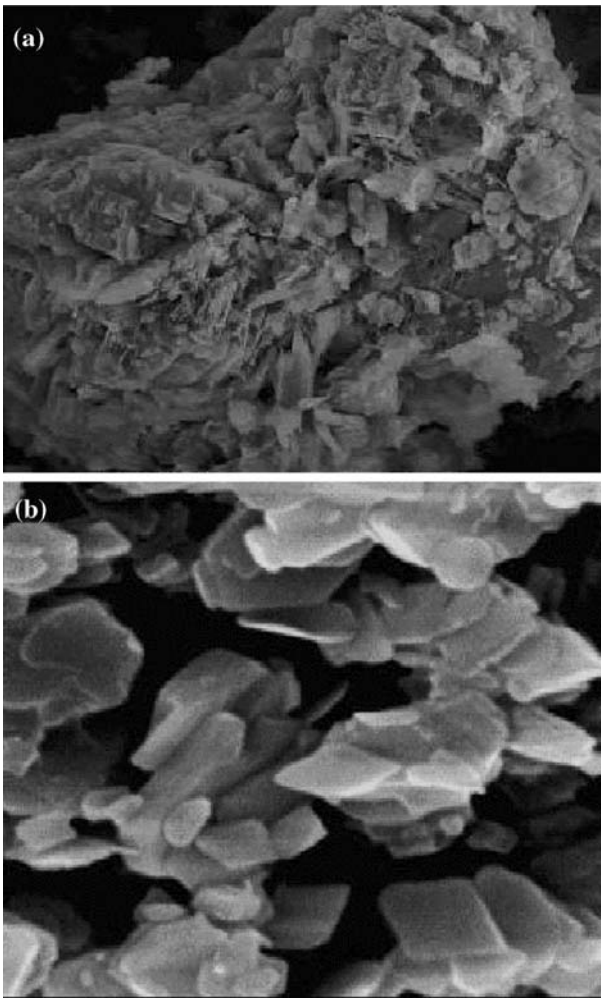

Figure 3. SEM micrographs for (a) VPH1 and (b) VPH2.

Compared to VPH1 catalyst, two differences from VPH2 can be observed. Firstly, the O_2 desorption profiles show an onset of O_2 evolution for VPH1 occurred at ~100 K higher than observed for VPH2. VPH1 also gave two overlapped peaks with their maxima located at 1035 and 1060 K which are higher compared to VPH2 catalyst with only one peak maximum appeared at 997 K. These results suggested that the oxygen species desorbed from VPH2 is likely to be more labile and reactive than those of VPH1 catalyst. Secondly, the amount of oxygen desorbed from the VPH2 catalyst is ~33 (3.38×10^{20} atom g^{-1}) higher compared to VPH1 catalyst (table 3). The lower desorption peak temperature and a higher total amount of oxygen desorbed suggested that VPH2 may possibly favour a higher

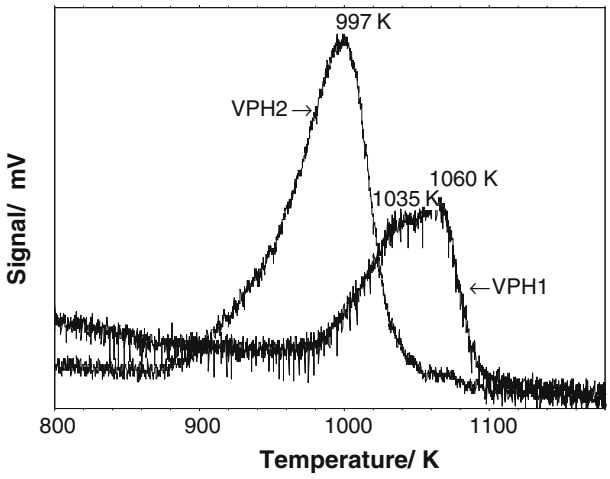

Figure 4. Temperature programmed desorption of O_2 from VPH1 and VPH2 catalysts.

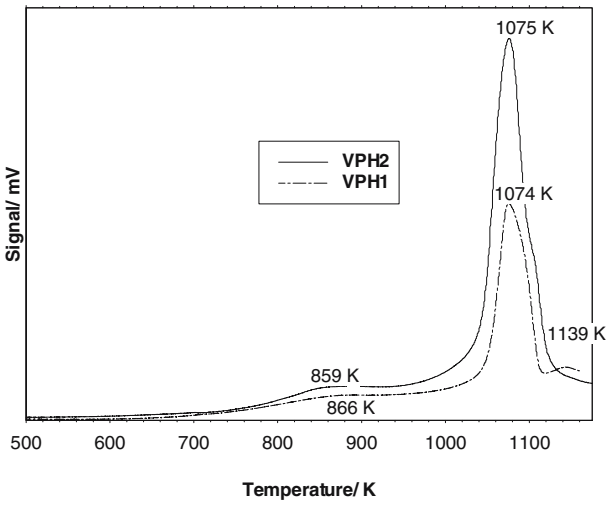

Figure 5. H_2 -TPR profiles of VPH1 and VPH2 catalysts.

activity attributed by a lower desorption activation energy required for removal of more oxygen atoms from the lattice.

3.5. Temperature-programmed reduction (TPR)

The surface reactivity of the catalysts was investigated by temperature-programmed reduction in H_2/Ar stream (5% H_2 in Argon, 1 bar, 25 cm^3 min^{-1}). The rate of hydrogen consumption was monitored by a thermal conductivity detector while raising the sample temperature from ambient temperature to 1173 K at 10 K min^{-1}.

TPR profiles (figure 5) show that VPH1 gave three reduction peaks observed at 866, 1074 (major peak) and 1139 K. However VPH2 gave two peaks maxima occurred at 859 and 1075 K. The reduction patterns for both catalysts are significantly different from that obtained for VPO [10] and VPD methods [13]. The first reduction peak appeared at higher temperature and the major reduction peak appeared as a sharp peak at ~1074 K and occurred at higher range of temperature (1000–1100 K) compared to VPO and VPD catalysts which exist as a broad peak at lower temperature (900–1060 K) [10,13].

The total amount oxygen species removed from VPH1 is 1.96×10^{21} atom g^{-1}. However, for VPH2, the total amount was increased to 3.28×10^{21} atom g^{-1} mainly contributed by the remarkably increased of the oxygen species from the major reduction peak (with 2.74×10^{21} atom g^{-1} compared to 1.35×10^{20} atom g^{-1} for VPH1). This particular oxygen is associated to V^{4+} phase [14] which is the active phase of the catalyst. A significant increase of reactive oxygen removed from the major peak of VPH2 suggested that this catalyst will obtain a higher C_4 conversion compared to VPH1 (table 4).

3.6. Oxidation of n-butane to maleic anhydride (1.7% n-butane in air, GHSV: 2400 h^{-1}, 673 K)

It is apparent that the improved hydrothermal synthesized catalyst (VPH2) produces higher activity (35%), which has comparative performance with the VPH1 catalyst (7%). The space time yield of VPH2 is also higher than VPH1. The MA selectivity obtained is 70 and 61% for VPH1 and VPH2, respectively (table 5). The enhancement in activity was due to the smaller crystallite size contributed to a higher surface area and also to the superior oxidant's nature with more active

Table 3
O_2-TPD data obtained from VPH1 and VPH2

Catalyst[a] (peaks)	T_{max}/K	Desorption activation energy, E_d (kJ mol^{-1})	Oxygen atoms desorbed from the catalyst (mol g^{-1})	Oxygen atoms desorbed from the catalyst (atom g^{-1})	Coverage[b] (atom m^{-2})
VPH1					
1	1035	285	2.07×10^{-4}	1.25×10^{20}	1.55×10^{19}
2	1060	292	1.69×10^{-4}	1.02×10^{20}	1.26×10^{19}
Total oxygen atoms desorbed			3.76×10^{-4}	2.27×10^{20}	2.81×10^{19}
VPH2	997	275.2	5.62×10^{-4}	3.38×10^{20}	3.56×10^{19}

[a] Surface area: VPH1 = 8.07 m^2 g^{-1} and VPH2 = 9.47 m^2 g^{-1}.
[b] The "coverage" is calculated by dividing the number of oxygen atoms removed (atom g^{-1}) by the specific surface area.

Table 4
Total number of oxygen atoms removed from the VPH1 and VPH2 catalysts by reduction in H_2/Ar

Catalyst[a] (peaks)	T_{max}/K	Reduction activation energy, E_r (kJ mol^{-1})	Oxygen atoms removed from the catalyst (mol g^{-1})	Oxygen atoms removed from the catalyst (atom g^{-1})	Coverage[b] (atom cm^{-2})
VPH1					
1	866	144.8	8.96×10^{-4}	5.39×10^{20}	6.67×10^{19}
2	1074	179.6	2.14×10^{-3}	1.29×10^{21}	1.60×10^{20}
3	1139	190.4	2.24×10^{-4}	1.35×10^{20}	1.67×10^{19}
Total oxygen atoms removed			3.26×10^{-3}	1.96×10^{21}	2.43×10^{20}
VPH2					
1	859	143.6	9.06×10^{-4}	5.45×10^{20}	5.76×10^{19}
2	1075	179.7	4.55×10^{-3}	2.74×10^{21}	2.89×10^{20}
Total oxygen atoms removed			5.35×10^{-3}	3.28×10^{21}	3.46×10^{20}

[a] Surface area: VPH1 = 8.07 m^2 g^{-1} and VPH2 = 9.47 m^2 g^{-1}.
[b] The "coverage" is calculated by dividing the number of oxygen atoms removed (atom g^{-1}) by the specific surface area.

Table 5
Catalytic performance of VPH1 and VPH2 for the oxidation of *n*-butane to maleic anhydride[a]

Catalysts	*n*-Butane conversion (%)	Maleic anhydride selectivity (%)	10^{-5} Space time yield (mol MA/(m^2 h))
VPH1	7	70	0.74
VPH2	35	61	2.96

[a] Reaction condition: 673 K, 1.7% *n*-butane in air, GHSV: 2400 h^{-1}.

and labile lattice oxygen as observed from the O_2-TPD and TPR spectra. A larger amount of oxygen atoms desorbed and removed originated from V^{4+} phase mainly contributed to the enhancement of the *n*-butane conversion. A small increment of V^{5+} phases (from 23% of VPH1 to 35%) of VPH2 was also favoured the activation of the butane [15]. A combination of $(VO)_2P_2O_7$ and an appropriate amount of α_{II}-$VOPO_4$ in the VPH2 catalyst lead to the enhanced catalytic performance for *n*-butane oxidation. However, the reducibility behaviour might also explain the lower *n*-butane conversion of both VPH1 and VPH2 as compared to other methods preparation of VPO catalyst [11,13]. High onset and reduction peak temperatures of the oxygen species removed from the active V^{4+} phase concluded that their oxygen species are less reactive.

Acknowledgements

Financial assistance from Malaysian Ministry of Science, Technology and Innovation is gratefully acknowledged.

References

[1] G.J. Hutchings, C.J. Kiely, M.T. Sananes, A. Burrows and J.C. Volta, Catal. Today 40 (1998) 273.
[2] C.J. Kiely, A. Burrows, S. Sajip, G.J. Hutchings, M.T. Sananes, A. Tuel and Volta, J. Catal. 162 (1996) 31.
[3] R.P. Unnikrishnan, S.D. Endalkachew and S.V. Rajender, Appl. Catal. A: General 252 (2003) 1.
[4] L. Mahony, D. Zemylyanov, E.S. Mark and B.K. Hodnett, Appl. Catal. A: General 251 (2003) 327.
[5] C.C. Torardi and J.C. Calabrese, Inorg. Chem. 23 (1984) 1308.
[6] J.K. Bartley, J.A.L. Sanchez and G.J. Hutchings, Catal. Today 81 (2003) 197.
[7] D. Fratzky, Th. Götze, H. Worzala and M. Meisel, Mat. Res. Bull. 33 (1998) 635.
[8] M. Niwa and Y. Murakami, J. Catal. 76 (1982) 9.
[9] G.J. Hutchings, J. Mater. Chem 14 (2004) 3385.
[10] Y.H. Taufiq-Yap, M.H. Looi, K.C. Waugh, M.Z. Hussein, Z. Zainal and R. Samsuddin, Catal. Lett. 74 (2001) 99.
[11] Y.H. Taufiq-Yap, M.H. Looi, M.Z. Hussein and Z. Zainal, Asian J. Chem. 14 (2002) 1494.
[12] P.H. Klug and E. Alexander, *X-Ray Diffraction Procedures for Polycrystalline and Amorphous Materials,* 2nd ed. (Wiley, New York, 1974).
[13] Y.H. Taufiq-Yap, K.P. Tan, K.C. Waugh, M.Z. Hussein, I. Ramli and M.B. Abdul Rahman, Catal. Lett. 89 (2003) 8.
[14] B.T. Pierini and E.A. Lombardo, Mat. Chem. Phys. 92 (2005) 197.
[15] G.W. Coulston, S.R. Bare, H. Kung, K. Birkeland, G.K. Bethke, R. Harlow, N. Herron and P.L. Lee, Science 275 (1997) 191.